

Indoor Optical Wireless Systems: Technology, Trends, and Applications

Ton Koonen , Fellow, IEEE, Fellow, OSA

(Tutorial Review)

Abstract—Indoor wireless traffic is evolving at a staggering pace, and is quickly depleting radio spectrum resources. Optical wireless communication (OWC) offers powerful solutions for resolving this imminent capacity crunch of radio-based wireless networks. OWC is not intended to fully replace radio wireless techniques such as WiFi, but to complement these and offload their high traffic loads. After discussing OWC's application domains, this paper gives a tutorial overview of two major directions in OWC: wide-coverage visible light communication which builds on LED illumination techniques and shares capacity among multiple devices, and communication with narrow 2-D steered infrared beams which offers unshared high capacity to devices individually. In addition, supporting techniques for wide field-of-view receivers, device localization, bidirectional hybrid optical/radio networks, and bidirectional all-optical wireless networks are discussed.

Index Terms—Diffraction grating, free-space optical receiver, hybrid network, indoor communication, localization, optical beam steering, optical wireless communication.

I. INTRODUCTION

ALREADY since decades, the demand for wireless communication is growing relentlessly. The growth is being fueled by broadband mobile services to smartphones, tablet computers, laptops, etc., and by interaction over the internet among the myriads of devices constituting the Internet of Things. These wireless traffic loads are mainly generated indoors, and are driving today's wireless networks such as those in the IEEE802.11 suite into serious congestion. New radio spectrum bands are being opened, e.g., sub-THz ones stretching the spectrum upto some 300 GHz. Nevertheless, this ongoing exponential traffic growth is quickly exhausting the capabilities offered by radio communication. In the optical domain, however, without requiring licensing fees in the vast frequency regions of the optical domain a wealth of additional spectrum is available, which can be disclosed by Optical Wireless Communication (OWC) techniques. Moreover, OWC enables to create smaller

Manuscript received October 28, 2017; revised December 21, 2017; accepted December 21, 2017. Date of publication December 26, 2017; date of current version March 1, 2018. The work of T. Koonen and co-workers was supported by the European Research Council under the Advanced Grant project "BROWSE-Beam-steered reconfigurable optical wireless system for energy-efficient communication".

The author is with the Institute for Photonic Integration, Eindhoven University of Technology, Eindhoven 5612 AZ, The Netherlands (e-mail: a.m.j.koonen@tue.nl).

Color versions of one or more of the figures in this paper are available online at <http://ieeexplore.ieee.org>.

Digital Object Identifier 10.1109/JLT.2017.2787614

communication cells in the network, which is a vital key to unlock the path to exponential capacity growth. According to Cooper's Law [1], the density of radio communications has increased with a factor of 10^6 in the past 45 years. To this factor, the opening-up of new radio spectrum has contributed with a factor 25, frequency division techniques with a factor 5, more comprehensive modulation formats with a factor 5, but the major factor ($1600\times$) was contributed by the introduction of spatial division, in particular by smaller cells enabling spectrum re-use.

OWC can offload heavy traffic loads from congested radio-based wireless networks, thus making the room available desperately needed for intense low-capacity streams such as in the Internet of Things. However, OWC is not intended to fully replace radio wireless communication; e.g., it cannot reach out-of-sight devices (such as smartphones etc. shielded within clothing), while radio techniques (below 60 GHz) can do that.

This paper intends to give a tutorial overview of the research domain of OWC. This field is very broad, with a large diversity of activities. The overview given therefore cannot be exhaustive, and mainly focuses on OWC techniques for short range (indoor) communication. After discussing the application domains of OWC, techniques for visible light communication (VLC) and for beam-steered infrared light communication (BS-ILC), which are the two main methods for OWC, are discussed. Subsequently, techniques for OWC receivers and for the localization of the users' devices are addressed. Finally, the application of these techniques in hybrid networks (i.e., combining optical wireless and radio wireless), and in all-optical OWC networks is discussed.

II. OWC'S APPLICATION DOMAINS

OWC is not hampered by electro-magnetic interference nor does it generate interference for EM-sensitive devices, it is nearly impossible to jam and offers a high level of privacy (e.g., does not penetrate walls), its installation can be relatively easy, and it gives access to a huge license-free spectrum. Building on its ability to selectively cover small areas, by means of spatial re-use it can offer a large aggregated capacity. These characteristics are advantageous in densely-populated environments where people generate high traffic loads, such as in open office rooms, conference halls, exhibition halls, airplane cabins, train cabins, (virtual reality) gaming halls, etc. Its relative ease of installation (e.g., VLC may be integrated with lighting) and high privacy level makes it attractive for residential services at home. Its

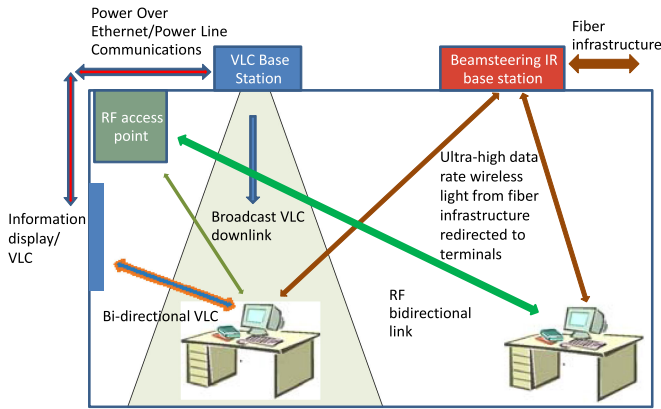


Fig. 1. Basic indoor OWC scenarios (from [2]).

EMI-insensitivity enables robust highly-reliable communication such as needed for industrial manufacturing robots, intra-data center top-of-the-rack interconnects, temporary (disaster-recovery) networks, etc. Atmospheric conditions may hamper its use for outdoors, in particular over longer reaches and in foggy conditions. Mobile backhauling for small radio cells (spaced several hundreds of meters), car-to-car and car-to-roadside communication are examples of attractive outdoor scenarios.

III. INDOOR OWC TECHNIQUES

As illustrated in Fig. 1, two major categories of indoor OWC techniques may be distinguished: visible light communication (VLC) and beam-steered infrared light communication (BS-ILC).

VLC (and more specifically LiFi [3]) gives access to no less than 320 THz in the 400–700 nm range. VLC typically is deployed in conjunction with illumination, by modulating the data on the LED luminaries. The re-use of the existing infrastructure can lower the entry threshold for VLC. These LEDs have primarily been designed for generating light in the most efficient way, and have a restricted modulation bandwidth. Moreover, the illumination systems typically serve a large area in which multiple devices have to share this limited VLC capacity by means of a suitable medium access control (MAC) protocol. The received light intensity goes down with the squared distance to the LED source, thus limiting the SNR and hence the reach. VLC requires that the illumination is switched on, which may not always be desired (e.g., when the room is already filled with bright daylight).

Beam-steered IR light communication (BS-ILC) brings the light only there where and when needed. It operates independently from illumination systems, and needs a separate infrastructure. Benefiting from well-established S+C+L band technologies for fiber-optic communication, access can be obtained to 20.9 THz in the 1460–1625 nm range. Multiple beams may each serve a user terminal within the room, without sharing. No MAC protocols to arrange shared access are needed. Hence each terminal can get a guaranteed capacity without conflict with other terminals. The directivity of a beam implies that the received power can be substantially higher than with VLC, enabling a higher SNR and thus a higher data rate and longer reach

TABLE I
OWC COMPARED WITH IEEE802.11 SUITE

	VLC	BS-ILC	WiFi IEEE802.11
Cap. per user	Shared; 9.5Gbit/s over 1m	Unshared; very high (up to 112Gbit/s per beam)	Shared; 802.11n (2.4GHz): <600Mbit/s 802.11ac (5GHz): <6.93Gbit/s 802.11ad (60GHz): <7Gbit/s
Reach	Short-medium (few m) Needs LoS	Medium (<10m)-long Needs LoS	Medium Does not need LoS (<60GHz)
Energy consumption	High (Watts); illumination needs to be on	Low (per beam, <10mW), on-demand only	Base station >100mW
Carrier freq., av. bandwidth	400-700nm; width 320THz	1460-1625nm (S+C+L bands); width 20.9THz	2.4GHz band; width 83.5MHz channels 20 or 40MHz 5GHz band; width 575MHz channels 20 or 40 or 80MHz 60GHz band; width 7GHz
Safety aspects	Penetrates eye If collimated: <1mW	Does not penetrate eye; collimated <10mW	EM hypersensitivity issues
Privacy	Moderate (visible light contained by walls; widely spread; may leak through windows; needs encryption)	Good (IR light contained by walls; directive; IR reflection coating can prevent leaks through windows)	Open; needs encryption
Infrastructure	Share LED illumination	New indoor (fiber) infra	Electrical cable (Cat5) infra
Standardisation	First steps made IEEE 802.11 LC study group	Not yet	Extensive, mature, keeps evolving Backwards compatible
Utilisation	First products on market	Laboratory phase	Very wide-spread, more WiFi devices than people on earth; >50% of internet traffic through WiFi

at better power efficiency. Moreover, IR light does not reach the vulnerable retina in the human eye, which implies that relatively high transmitted power levels are allowed within the eye safety limits (up to 10 mW for $\lambda > 1.4 \mu\text{m}$, according to IEC 60825, ANSI Z136 standards [4]). Furthermore, a photodiode’s responsivity basically is proportional to wavelength, which at high data rates yields higher-sensitivity receivers in the IR domain than in the visible domain.

The IEEE802.11 suite of radio standards is presently widely used for indoor wireless communications. Its basic characteristics are compared in a non-exhaustive way with exemplary OWC characteristics in Table I. With BS-ILC, no capacity sharing is incurred, thus a guaranteed very high capacity per device can be provided. With both VLC and BS-ILC, however, line-of-sight (LoS) is needed, whereas with the IEEE802.11 radio techniques below 60 GHz also non-LoS devices can be reached.

Products of the 802.11 suite are abundantly available commercially, whereas VLC is bringing some first products into the market and BS-ILC is still largely in the laboratory research phase. Due to the difference in market maturity, cost comparisons are hard to make. Basically, from a capital expenditures (CAPEX) perspective the 802.11 suite and VLC tend to incur lower costs, as they need little infrastructure or re-use existing infrastructure (by means of powerline communication, or power-over-ethernet techniques), while BS-ILC needs a new fiber infrastructure. From the perspective of the recurring operating expenditures (OPEX), the BS-ILC may be more beneficial as it can be more energy-efficient due to its capability to offer capacity-on-demand.

IV. VISIBLE LIGHT COMMUNICATION TECHNIQUES

LEDs which are primarily designed for illumination purposes typically deploy a blue LED chip plus a phosphor coating which generates the white light (see Fig. 2(a) [5]). The slow decay time of the phosphor severely limits the bandwidth to a few MHz only. Some improvement is obtained when filtering the blue LED light at the receiver, but the bandwidth is still restricted (typically <20 MHz). Employing this blue-filtering and basic NRZ-OOK

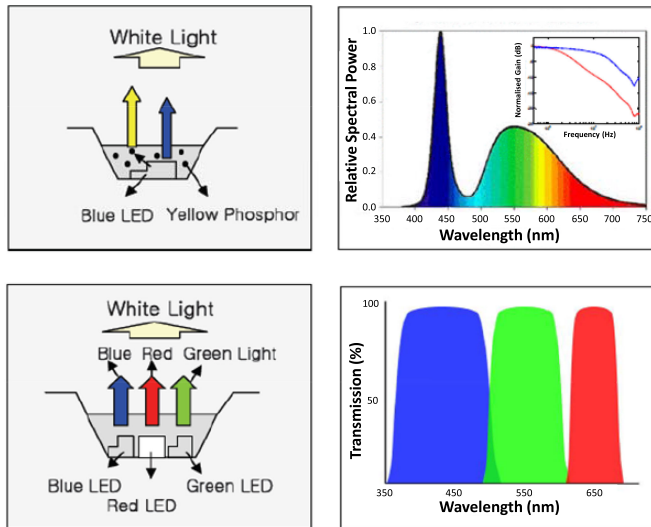


Fig. 2. LED types for VLC: (a) blue LED + phosphor and (b) RGB multi-element LED [5].

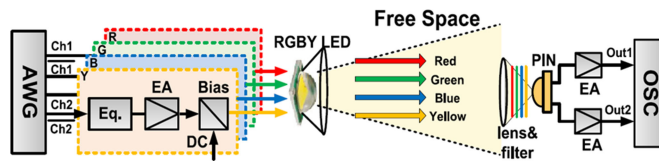


Fig. 3. 8 Gbit/s quad-color VLC system using CAP modulation [9].

modulation, 40 Mbit/s transmission has been achieved at an illumination level of 700 lx (office areas require 200–800 lx) [6]. Spectrum-efficient advanced modulation schemes are to be used in order to realize higher data rates. Applying OFDM with 256 subcarriers and bit-loading, in conjunction with a pre-equalizing filter before the LED driver and a blue filter before a PIN-TIA receiver, a net data rate of 2.0 Gbit/s over 1.5 m free-space reach was achieved, and 0.79 Gbit/s over 3 m [7].

Alternatively, white light may be produced by a multi-element LED, composed of tri-color elements (red + green + blue; see Fig. 2(b) [5]). Although each of the LED elements may have a limited bandwidth (typically some 15 MHz), by modulating them separately the capacity can be tripled. The wavelength division multiplexing (WDM) approach requires a more complex driver at the transmitter end, and three color-filtering stages in parallel at the receiver. Taking this approach, and using DMT modulation with 512 subcarriers and color-filtering APD receivers, 3.4 Gbit/s was achieved over 10 cm (at 410 lx), and 2.2 Gbit/s over 30 cm (at 25 lx) [8]. With a quad-color LED (red + green + blue + yellow) and tailored CAP modulation (128-CAP for red, 32-CAP for green, 64-CAP for blue, 128-CAP for yellow), an aggregate capacity of 8Gbit/s over 1m was achieved (see Fig. 3) [9].

The integration of lighting and communication functions brings particular challenges, as the consumer should not perceive any light flickering effects and dimming the light over a wide range should be possible, while communication should continue to be supported. Within IEEE 802.15.7, standards are set for high-speed VLC up to 96 Mbit/s. Among their physical

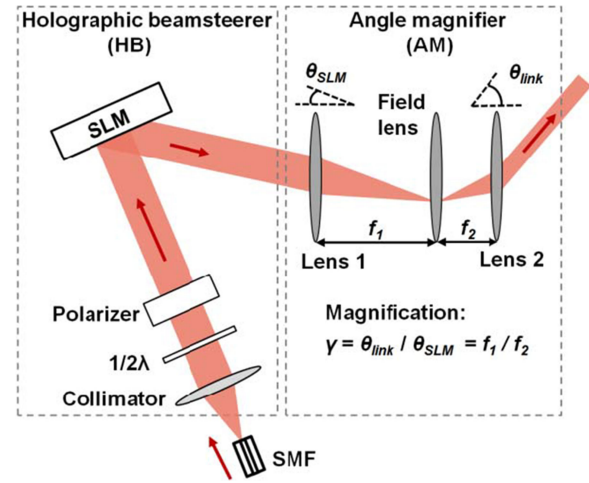


Fig. 4. 2D beam steering with SLM and angle magnifier [18].

layer techniques is the use of multi-color sources using color shift keying (CSK) [10]. Multi-color CSK schemes using three colors (RGB) and four colors (blue, cyan, yellow, red) have been proposed; the four-dimensional coding scheme can have a higher efficiency and better reliability for a given multipath delay spread [11]. CSK uses intensity-modulation of the individual colored LED elements, which implies that the resulting overall color is varying quickly. These instantaneous color variations should not be perceivable by the human eye, so should be faster (i.e., <10 ms) than the critical flicker fusion threshold and the critical color fusion threshold. The transmission by the multi-color LED should be set such that when time-averaged a specific constant color is perceived, which requires adequate LED-driving algorithms [12].

Yet another approach is to apply an array of micro-LEDs, which each due to their small active area can have a large bandwidth. Using an array of blue ($\lambda = 420$ nm) GaN μ LEDs each having an active area diameter of only 42 μ m, bandwidth of 400 MHz, and 5.7 mW output power, with PAM-4 modulation 3.8 Gbit/s (3.5 Gbit/s excluding 7% FEC) over 0.75 m was achieved, and 5.37 Gbit/s (5 Gbit/s excl. FEC) when using DCO-OFDM with 512 bit-loaded subcarriers [13].

Spatial multiplexing can open another route towards higher VLC capacity. In a MIMO system setup with a 2-dimensional array of 9 individually addressable $\varnothing 39$ μ m blue GaN μ LEDs emitting at $\lambda = 450$ nm and with 9 APDs (each 200×200 μ m², bandwidth >90 MHz) made in a 0.18 μ m CMOS process, with PAM-8 modulation about 890 Mbit/s per channel was achieved over a free-space link of 50 cm, and an aggregate rate of 6.95 Gbit/s (excl. 7% FEC) [14].

VLC systems are becoming available commercially. Bi-directional point-to-point systems are offered providing 1 Gbit/s connectivity with low latency (<2 ms) [15]. Dubbed LiFi, VLC techniques (which are basically point-to-point) are extended into a fully networked system in an atto-cells network architecture, supporting seamless handover between these cells and bi-directional operation [3]. The LiFi-X system of PureLiFi supports 40 Mbit/s full-duplex communication, using a USB dongle at the user's device [16].

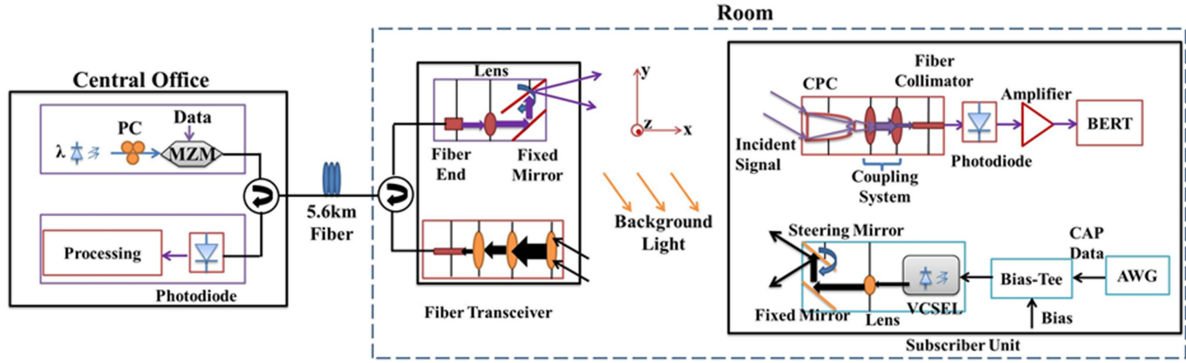


Fig. 5. 2D beam steering with MEMS mirrors [20].

V. BEAM-STEERED IR LIGHT COMMUNICATION TECHNIQUES

When working with narrow IR beams, accurate and independent two-dimensional steering of multiple beams is needed in order to establish links to multiple (non-stationary) terminals. First concepts for this were introduced in [17], describing beam steering by a material in which multiple holograms were recorded. By using a specific spatial code on the beam which is impressed by means of a spatial light modulator (SLM), the beam is deflected by the corresponding hologram into a specific direction.

Several approaches can be followed to establish beam steering, which may be classified coarsely in those using active steering devices and in those using passive ones.

A. Active Beam-Steering Devices

In active beam steering devices (e.g., MEMS mirrors, spatial light modulators (SLMs)) the state of the device is changed by means of a separate control channel, and a change in the state implies a change in the beam's direction. Per beam a separate controllable state is needed, which compromises scaling to many beams.

An SLM having 512×512 pixels with 256 phase levels was used for steering a beam at $\lambda = 1.55 \mu\text{m}$ (see Fig. 4) [18]. The maximum steering angle θ_{max} attainable by the SLM is determined by the SLM's pitch p ; with a $p = 15 \mu\text{m}$, this was only $\theta_{\text{SLM,max}} = \lambda/2p \approx 3^\circ$. An angular magnifier composed by an afocal system with 2 lenses having focal lengths f_1 and f_2 was applied, and can yield an angular magnification factor $\gamma = \theta_{\text{link}}/\theta_{\text{SLM}} = f_1/f_2$, which inevitably goes together with a beam narrowing factor f_2/f_1 . A third lens may be put in between to reduce lens aberrations. Using such angular magnifier with effective $\gamma = 10$, steering was achieved over $\theta_{\text{link}} = 30^\circ$. Operating in WDM mode with 3 channels spaced by 10.1 GHz and carrying 16-QAM signals, $3 \times 37.4 \text{ Gbit/s} = 112 \text{ Gbit/s}$ (incl. 7% FEC) over a 3 m free-space link was achieved. If its aperture allows, a SLM may also be operated in different zones each steering a beam [19]. Thus multiple beams can be steered by a single SLM, and optionally point-to-multipoint communication can be supported by sharing different zones.

By means of MEMS mirrors, 2D steering over relatively large angles can be achieved. In [20], steering over $>20^\circ$ is reported,

providing 10 Gbit/s with CAP-16 modulation over 2 m downstream communication with 7 mW launched power at $\lambda = 1551 \text{ nm}$ (see Fig. 5). A compound parabolic reflector (CPC) was used to increase the receiving aperture, followed by a fiber collimator and PIN photodiode receiver. Deploying a similar MEMS steering mirror and VCSEL emitting 5 mW at $\lambda = 850 \text{ nm}$, in the upstream direction 2 Gbit/s was transmitted.

B. Passive Beam-Steering Devices

Alternatively, the beam steering can be done by passive devices, which do not change state and have no moving parts. These devices do not need local powering nor a separate control channel. Such passive function may be implemented by a diffractive device, through which the beam steering is controlled by changing the wavelength of the optical data signal fed to the device [21]. The control is thus embedded in the data signal and no separate control channel is needed, which simplifies the network's architecture and the system's management. The optical data signals are fed to the steering device by means of an indoor fiber network, and are generated by wavelength-tunable laser transmitters. These transmitters may be jointly located and controlled in a centralized site, which eases maintenance and upgrading of the network. Laser tuning times are typically much less than tuning times of a MEMS mirror or SLM, and therefore the beam steering process can be much faster.

Diffraction gratings are well known for deflecting a light beam at an angle ψ as a function of the beam's wavelength λ . The beam steering is governed by the classical grating equation $\sin \psi + \sin i = m \cdot \lambda / (n \cdot d)$ where i is the beam's incident angle on the grating, m is the order of interference, d is the grating's period, and n the refractive index of the outside medium [22]. The beam is typically deflected in multiple orders m . The free spectral range (FSR) of order m , indicates the width of the wavelength range $\Delta\lambda_{\text{FSR},m}$ for which a beam does not enter a neighboring order. From the grating equation, it can be derived that $\Delta\lambda_{\text{FSR},m} = \lambda_1 / (m - 1)$ where λ_1 is the lowest wavelength of the wavelength range, and that the angular dispersion is $d\psi/d\lambda = m / (n \cdot d \cdot \cos \psi)$. For the maximum angular tuning range $\Delta\psi_{\text{max}}$ which can be achieved when tuning the wavelength over the full FSR $\Delta\lambda_{\text{FSR},m}$, it is found that $\cos \Delta\psi_{\text{max}} = 1 - (\lambda/d) \cdot (m / (m - 1))$ [21]. Hence, in order

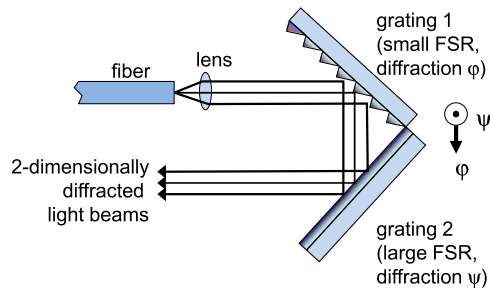


Fig. 6. 2D beam steering with two crossed gratings [26].

to achieve a relatively large angular tuning, a large order m and small grating groove spacing d are needed. E.g., when deploying a tuning range from $\lambda = 1500$ to 1600 nm, it is found that at $m = 16$ a $\Delta\psi_{\max} = 28.36^\circ$ is achieved for a grating with 75 grooves/mm and a large incidence angle of 66.93° .

1-Dimensional (1D) beam steering with a plane reflection grating was introduced in [23] for fast optical scanning applications. It was applied for steering of 3.3 mm diameter beams transmitting 10 Gbit/s with OOK modulation over 2.5 m in [24], employing an echelle grating of 79 grooves/mm, with blaze angle of 75° . An angular steering range of $\Delta\psi = 17.2^\circ$ was achieved when tuning over 130 nm from $\lambda = 1500$ to 1630 nm in orders $m = 15$ and $m = 16$. Upscaling the system to steer multiple beams can be achieved without changing the diffractive device; it just requires that multiple wavelengths are fed to the device, where each wavelength independently determines the direction of its beam.

For 2D optical scanning, it was proposed to create a number of tilted narrowband Bragg gratings in a photo-thermo-refractive (PTR) glass volume [25]. Each grating directs the beam with the wavelength which matches that grating into a specific direction. 2D scanning with $M \times N$ beams may be achieved by N PTR plates with each M tilted gratings. Experimentally, a scan over 5° was shown with 4 tilted Bragg gratings at 816 lines/mm when tuning the wavelength over 80 nm. For 2D steering which can be scaled to an arbitrary number of beams, it was proposed to use two crossed diffraction gratings (see Fig. 6) [26]. The first grating has a small FSR and many orders of this grating are traversed when tuning the wavelength over the full system range $\Delta\lambda_{\text{tun}}$. The second grating has an FSR which is at least $\Delta\lambda_{\text{tun}}$. As a result, a full line-by-line scanning of a 2D area takes place when tuning the wavelength of the beam over $\Delta\lambda_{\text{tun}}$: the beam is quickly steered along the diffraction direction of the first grating, and slowly along the orthogonal diffraction direction of the second grating. An arbitrary number of beams can independently be steered by feeding an equal number of wavelengths. With 2 crossed reflection gratings with 31.6 and 79 grooves/mm respectively, 2D angular beam steering over $5.6^\circ \times 14^\circ$ was achieved when tuning the wavelength from 1529 to 1611 nm [27]. Over a free-space link of 2.5 m with a beam diameter of 3.3 mm and path loss up to 14.6 dB (including SMF-coupled lens collimators), 42.8 Gbit/s was transmitted using DMT modulation. With a cross-aligned combination of a transmission grating of 1000 grooves/mm operating in order

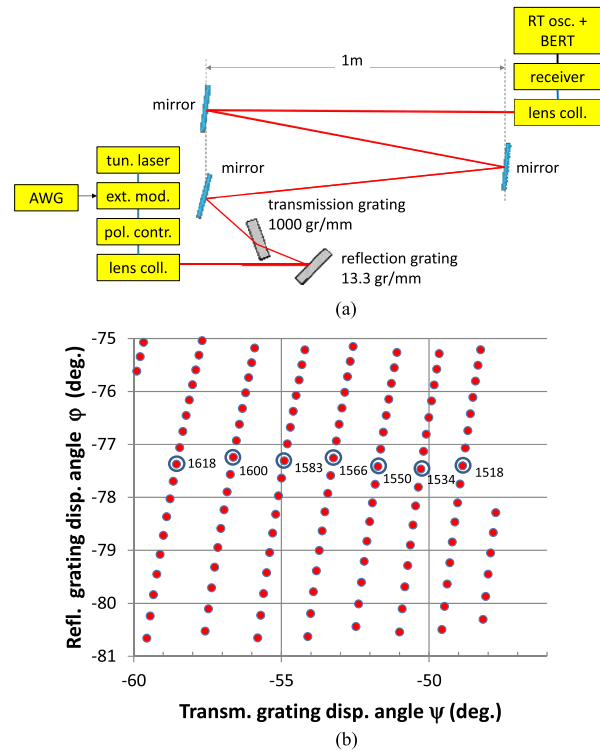


Fig. 7. 2D beam steering with crossed gratings [21]. (a) Setup with reflection and transmission grating. (b) Wavelength-controlled 2D scanning.

$m = 1$ and a reflection grating of 13.3 grooves/mm operating from order $m = 95$, 2D angular beam steering over $5.6^\circ \times 12.7^\circ$ was achieved when tuning from 1505 to 1630 nm for which 8 scanning lines were obtained (see Fig. 7) [21]. In combination with the SMF-coupled triplet lens collimators with 18.4 mm focal length, the -3 dB bandwidth of the pencil beam channel was found to be 10.35 GHz. The optical path losses were reduced to less than 6.15 dB, and by means of PAM-4 modulation 32 Gbit/s could be transmitted over a 3 m free-space link.

The crossed-grating concept can also be realized with a virtually imaged phased array (VIPA) as the element with a small FSR operating in high order m . A VIPA can be implemented by a glass plate with two parallel reflective sides, and its interference order m is about twice the optical thickness of the plate $n_v \cdot t$ divided by the wavelength λ . With a VIPA of $t = 100 \mu\text{m}$ thickness and refractive index $n_v = 1.5$ (so $m = 200$ at $\lambda = 1500$ nm), in combination with a transmission grating of 500 lines/mm, 2D line-by-line scanning over $5^\circ \times 9^\circ$ when tuning from 1400 to 1600 nm can be achieved [28].

A compact photonic integrated circuit (PIC) which can provide 2D beam steering using the cascaded-gratings concept has been reported in [29]. An arrayed waveguide grating was co-integrated with an array of waveguide grating couplers in a passive silicon-on-insulator technology; input-to-free-space losses were 8.9 to 10dB. 2D steering was achieved over $15^\circ \times 50^\circ$ by wavelength tuning over 100 nm; with a beam width of 4° , 50 resolvable spots could be generated in 2D. In [30], 2D beam steering by means of an active PIC implemented in InP technology has been reported. While using an on-chip SG-DBR laser

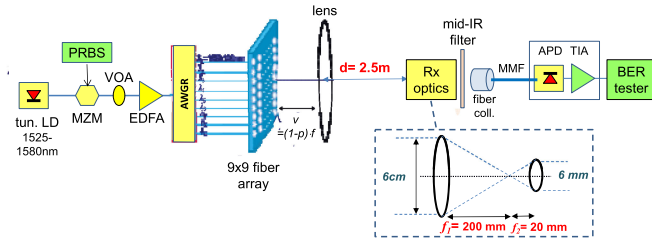


Fig. 8. 2D beam steering with high port-count AWGR [33].

diode with a wavelength tuning range beyond 30 nm, by tuning the wavelength as well as tuning electro-optically the local phase in the branches of an arrayed waveguide grating router 2D steering of a single beam over $3.5^\circ \times 10^\circ$ was achieved.

Stepwise wavelength-controlled 2D beam steering may be achieved by means of an arrayed waveguide grating router module which has a large number of output fiber ports. By arranging the output fibers in a 2D array, and putting this array in front of a lens, each output fiber launches a beam at its specific wavelength into a 2D angular direction given by the lateral position of that fiber with respect to the lens axis [31], [32]. In combination with the lens focal length, the pitch between the fibers in the 2D array is chosen such that the beams create adjacent spots in the 2D area to be covered. By putting the 2D fiber array slightly closer to the lens than its focal plane, the beams are slightly diverging and the module can be made more compact. When using a 1×80 ports AWGR, by applying a defocusing of 12%, the required lens focal length is 10 cm, its aperture 5.0 cm, and the fiber pitch in the 2D array is 3.7 mm. Transmission of 20 Gbit/s with NRZ-OOK modulation over 2.5 m was shown within the AWGR's -3 dB bandwidth of 35 GHz, while steering was achieved over $17^\circ \times 17^\circ$ when tuning over C-band (see Fig. 8) [33].

VI. OWC RECEIVER

As the OWC receiver is part of a user's device, it should be compact and low-cost, it should not require tedious alignment with respect to the downstream OWC transmitter, and it should capture enough optical power to enable a high downstream data capacity. Hence it should have a wide field-of-view (FoV) and a large aperture. However, increasing the active area of a photodetector is typically accompanied by a reduction of its bandwidth. The "conservation of etendue" law in physics states that etendue (a.k.a. $A \cdot \Omega$ product, the product of entrance area and solid angle subtended by a cone of light) is conserved when light travels through optical systems with perfect, loss-free reflections and refractions. Etendue can then remain constant or increase (e.g., by applying a diffuser), but not decrease [34]. With a compound parabolic reflector (a non-imaging optical element typically used for solar energy concentration [35]; cf. Fig. 5) put in front of a photodetector, the receiving aperture can be increased, but at the expense of a reduced FoV.

The effective detection area of the OWC receiver may be enlarged while maintaining adequate bandwidth by using a 2D array of fast photodiodes co-integrated with individual electrical preamplifiers followed by a summation amplifier. In [36], a

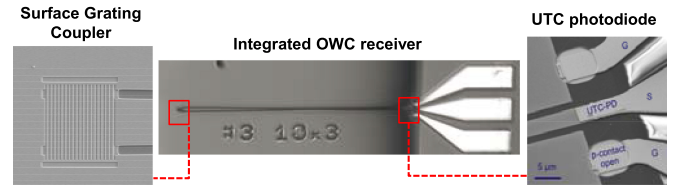


Fig. 9. Integrated cascaded aperture optical receiver [38].

2D array of 7 MSM hexagonal photodiodes is reported, each having a side length of $50 \mu\text{m}$ and 0.12 pF capacitance, followed by a current-summing amplifier, yielding an effective aperture diameter of $260 \mu\text{m}$ and overall -3 dB bandwidth of 3.7 GHz.

With a slab concentrator of which the slab waveguide is doped with fluorophore and is terminated with a photodetector, the link between the etendue of the light collection area and that of the detector can be broken [37]. The incoming light is converted to a longer wavelength by the fluorophore and guided to the detector by reflections at the slab surfaces; thus a wider FoV and higher gain is obtained. Using a quantum dot material as the fluorophore, a gain $50\times$ that of an etendue-preserving concentrator with the same FoV can be reached. The long slab may lead to channel dispersion effects, thus reducing the bandwidth and making this solution less suitable for high data rates.

Alternatively, in order to circumvent the compromise between aperture and bandwidth, the light collection function may be separated from the light detection function. Thus both functions may be optimized independently. Using InP photonic integration technology, a wide-area surface grating coupler (SGC) collecting the incident light has been monolithically integrated with an InP waveguide feeding a fast photodiode. A $10 \times 10 \mu\text{m}^2$ SGC was coupled via a narrow waveguide to a $3 \times 10 \mu\text{m}^2$ UTC photodiode which had an electrical bandwidth exceeding 67 GHz (see Fig. 9) [38]. With this integrated SGC-waveguide-PD device, free-space 40 Gbit/s NRZ-OOK data transmission has demonstrated. Without compromising the bandwidth, the light collecting aperture can be increased further by enlarging the SGC by means of apodization, and by creating an array of SGCs plus an on-chip light combiner.

VII. LOCALIZATION

Next to sending data for communication, a VLC system composed of (multiple) LED luminaries can send signals which contain the ID of the LEDs and with this can assist in determining the position of a device. As compared to RF, visible light suffers less from multipath effects, and can provide more accurate positioning. The location of the device may be determined by an algorithm using tri-angulation based on time-of-arrival (ToA, like in GPS) data of the light signals from various directions, on time difference of arrival (TDoA) data, on angle of arrival (AoA) data, or on received signal strength (RSS) data [39]. The ToA and TDoA methods require accurate synchronization. AoA can achieve the highest accuracy, but is the most complex to realize. RSS is the most popular in VLC systems as it operates asynchronously and is simple to implement, but it needs well-known path loss models. Alternatively, localization

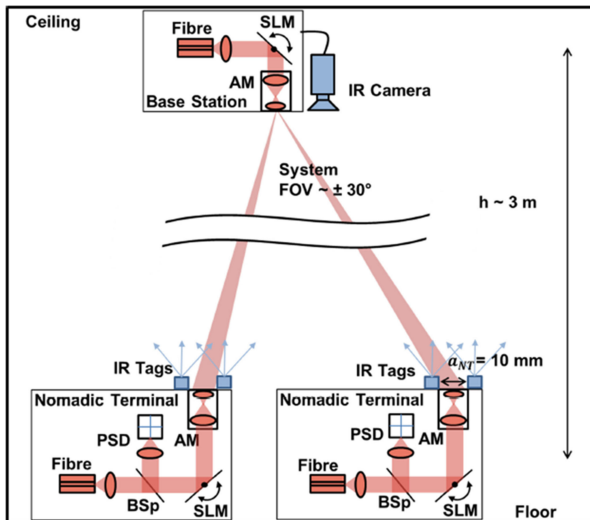


Fig. 10. Device localization using IR tags and a camera (AM: angular magnifier, BSp: beam splitter, PSD: position-sensitive detector) [45].

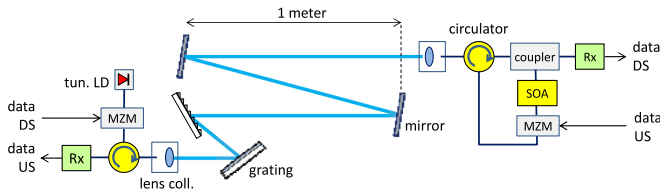


Fig. 11. Bi-directional all-optical wireless communication [46].

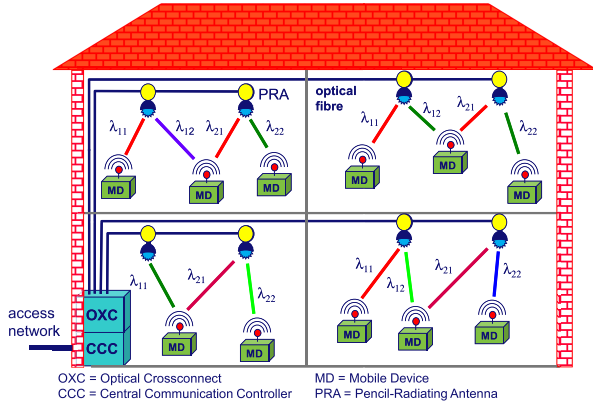


Fig. 12. Hybrid OWC/radio networking using wavelength-controlled 2D infrared steered beams [21].

may use an algorithm based on finger printing, or on vision analysis (using a camera at the device).

Optical Camera Communication (OCC) [40], [41] is being explored for low-to-moderate speed data transfer by LED lighting, and deploys an image sensor or camera at the user's device, e.g., in a smartphone. The data speed is basically limited by the camera's frame rate. MIMO techniques can be exploited using an LED array and image sensor with pixel-to-bit mapping. By means of computer vision analysis techniques which enable extraction of the LED coordinates, OCC can also enable accurate device positioning.

In [42], a 16×16 array of $100 \times 100 \mu\text{m}^2$ GaN μLEDs emitting at $\lambda = 450 \text{ nm}$ is used to generate a time sequence

of spatial illumination patterns. These patterns create a specific fingerprint optical signal sequence per site, which when detected by a simple photodetector can provide the device's location. Fast positioning within 10 ms was shown, with an accuracy better than 5 mm over 40cm distance; accuracy and area coverage can be improved when more emitters are used.

For beam-steered OWC, the position of the user's device needs to be known with an accuracy depending on the beam's width. For localizing and tracking a device in a hybrid system which uses beam-steered OWC techniques for downstream and radio techniques for upstream, WiFi positioning techniques may be deployed, or more accurately 60 GHz antenna pattern nulling. In [43], at the device side two high-gain horn antennas with 30 dBi gain are sending upstream data at 60 GHz, and RSS pattern nulling techniques at the central ceiling site are used to determine the device's location and direct the downstream optical beam accordingly (see Fig. 13). When using a 2D diffractive beam steerer (e.g., one based on a crossed grating pair, or high port-count AWGR, as discussed in Section V), the localization may be done by means of the wavelength-to-position mapping function of the steerer. The user's device may send light with a broad spectrum (such as ASE from an SOA) upstream, and the 2D diffractive beam steerer will pass a narrow slice of this upstream light. By assessing the wavelength of this slice with a sensitive spectrum analyzer, the location of the device can be determined [44]. Alternatively, at the ceiling a camera may be installed which when aided by vision analysis enables quick localization and tracking of the devices. A device may be equipped with a beacon which is traced by the camera. In [45], a circular array of 12 near-IR LEDs emitting at $\lambda = 890 \text{ nm}$ is used, mounted around the aperture of the optical receiver (see Fig. 10). The LEDs have a large emission half angle of 50° , which fits within the FoV's half angle of 30° of the system. By means of a CMOS wide-FoV camera, multiple devices can be localized with an accuracy of 0.05° (i.e., 2.5 mm at 3 m room height).

VIII. HYBRID OPTICAL/RADIO WIRELESS NETWORKS

Many network concepts reported focus on high-capacity downstream transmission using OWC and provide the upstream path by means of (established) lower-capacity radio techniques. The capacity asymmetry is acceptable in many service scenarios, such as the downloading of large video files, but may be inadequate for symmetric capacity needs such as fast bi-directional file transfer between data servers or computers.

A symmetric high-capacity full-duplex OWC system is shown in Fig. 11 [46]. Based on wavelength-controlled 2D beam steering with crossed gratings, it employs the principle of reversibility of an optical path when operated at the same wavelength. Fiber-pigtailed triplet lens collimators were used to send/receive beams with 3.3 mm diameter, and optical circulators at the central site and at the user's device site separate the up- and downstream signals. The downstream beam carries 10 Gbit/s OOK at a moderate optical extinction ratio of 3.6 dB. This enables the receiver at the device side to remove the modulation by means of an SOA operating in the gain-saturated regime, and to regain an almost clean optical carrier. This carrier is subsequently

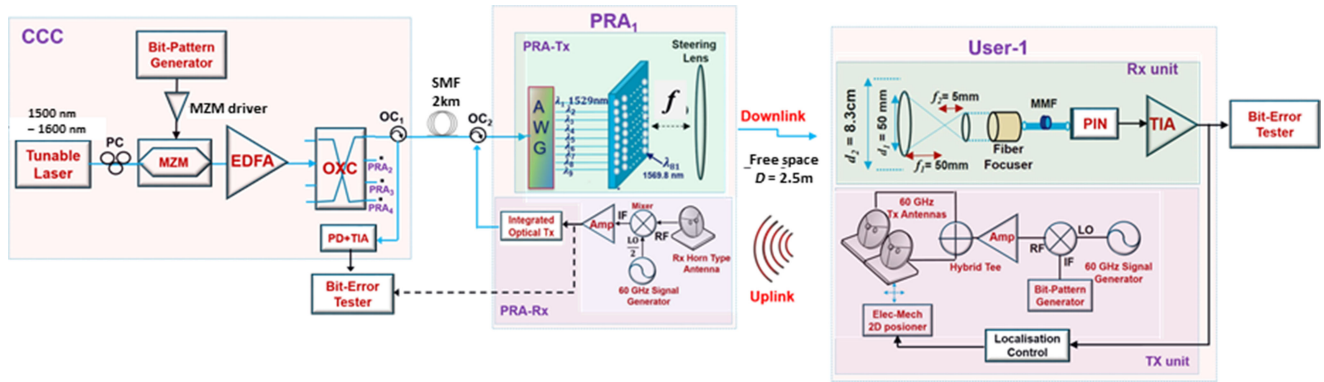


Fig. 13. Hybrid system with 2D beam-steered OWC downstream and 60 GHz-based radio communication upstream [43].

re-modulated by a Mach Zehnder Modulator (MZM) with 10 Gbit/s OOK upstream data. As the upstream signal thus has the same wavelength as the downstream signal, it takes the same path backwards through the crossed-gratings module.

Within the European Research Council's project BROWSE - Beam-steered Reconfigurable Optical-Wireless System for Energy-efficient communication, a hybrid OWC/radio network architecture is investigated as shown in Fig. 12 [21]. This architecture includes an indoor fiber backbone network, which flexibly routes the optical signals on-demand to the appropriate rooms by means of an optical crossconnect (OXC) at a centralized site in the building, governed by the intelligence in the central communication controller (CCC). Each room has a diffractive pencil-radiating antenna (PRA), which is fed by the fiber network and can steer multiple beams two-dimensionally in directions determined by their wavelengths. Each room should have multiple PRAs in order to resolve line-of-sight blocking. The upstream path from each mobile device (MD) is to be established with 60 GHz radio beams steered with phased array antennas. An integrated full-duplex hybrid system has been reported in [43] which provides 35 Gbit/s with OOK modulation downstream per infrared beam steered by a PRA composed of an 80-ports AWGR driving a 2D fiber matrix and $f = 40$ cm condenser lens structure (see Fig. 13). The beam diameter was 8.3 cm, and with a reach of 2.5 m, an angular coverage of $17^\circ \times 17^\circ$ was achieved. Upstream, 5 Gbit/s ASK was sent by 60 GHz radio beams, deploying two 30 dBi gain horn antennas at the device side and a 16 dBi antenna at the PRA side. The horn antennas were placed on a 2D electro-mechanical positioning stage, which enabled the device localization function. By applying PAM-4 modulation, the system's downstream throughput has been upgraded to 112 Gbit/s per beam [47].

IX. CONCLUDING REMARKS

Optical Wireless Communication techniques hold a great potential to resolve the imminent exhaustion of indoor wireless communication resources. The optical spectrum, both in the visible and in the infrared domain, offers ample extra bandwidth without licensing issues, and thus great opportunities for carrying large volumes of wireless traffic. OWC can thus off-load much of the burden on radio wireless networks. It will not

fully replace radio wireless communication (e.g., it cannot support services without line-of-sight), but it will complement and co-exist with it. First VLC products are entering the market in appealing applications. Beam-steered infrared communication techniques have shown their ability to offer ultra-high data rates (beyond 100 Gbit/s per beam). Considerable work is still to be done to bring these techniques to market maturity, e.g., research on compact low-cost OWC receivers, symmetric bi-directional OWC systems, scaling of coverage area and reach, efficient localization, and co-existence scenarios with radio wireless technologies. As OWC technologies have not matured yet, cost comparisons are hard to make. From a general viewpoint, VLC systems may be preferred regarding CAPEX due to their lower infrastructure costs, whereas BS-ILC systems may be more beneficial regarding OPEX due to their lower energy consumption.

ACKNOWLEDGMENT

The author thanks Dominic O'Brien, Volker Jungnickel, Harald Haas, Nan Chi, Sietse van der Gaast and many other colleagues in the OWC field for valuable discussions and inputs, and also the co-workers at TU/e in the BROWSE project Eduward Tangdionga, Zizheng Cao, Joanne Oh, Ketema Mekonnen, Fausto Gomez-Agis, Frans Huijskens, Xinran Zhao, Xuebin Zheng, Amir Khalid, Maria Torres Vega, Antonio Liotta, Bindi Wang, Peter Baltus, and Marion Matters.

REFERENCES

- [1] 2011. [Online]. Available: <http://www.arraycomm.com/technology/coopers-law/>
- [2] D. C. O'Brien, "Optical wireless communications: Current status and future prospects," in *Proc. IEEE Summer Top.*, Newport Beach, CA, USA, Jul. 11, 2016 (36 slides).
- [3] H. Haas, L. Yin, Y. Wang, and C. Chen, "What is LiFi?," *J. Lightw. Technol.*, vol. 34, no. 6, pp. 1533–1544, Mar. 2016.
- [4] 2017. [Online]. Available: https://en.wikipedia.org/wiki/Laser_safety
- [5] V. Jungnickel, "Optical wireless in 5G," in *Proc. IEEE Summer Top.*, Newport Beach, CA, USA, Jul. 11, 2016 (58 slides).
- [6] J. Grubor, S. C. J. Lee, K.-D. Langer, A. M. J. Koonen, and J. W. Walewski, "Wireless high-speed data transmission with phosphorescent white-light LEDs," in *Proc. 33rd Eur. Conf. Exhib. Opt. Commun. 2007*, Berlin, Germany, Sep. 16–20, 2007, Paper no. PD3.6.
- [7] X. Huang *et al.*, "2.0-Gb/s visible light link based on adaptive bit allocation OFDM of a single phosphorescent white LED," *IEEE Photon. J.*, vol. 7, no. 5, Oct. 2015, Paper no. 7904008, doi: [10.1109/JPHOT.2015.2480541](https://doi.org/10.1109/JPHOT.2015.2480541).

- [8] G. Cossu, A. M. Khalid, P. Choudhury, R. Corsini, and E. Ciaramella, "3.4 Gbit/s visible optical wireless transmission based on RGB LED," *Opt. Express*, vol. 20, no. 26, pp. B501–B506, Dec. 2012.
- [9] Y. Wang, L. Tao, X. Huang, J. Shi, and N. Chi, "8-Gb/s RGBY LED-based WDM VLC system employing high-order CAP modulation and hybrid post equalizer," *IEEE Photon. J.*, vol. 7, no. 6, Dec. 2015, Paper no. 7904507, doi: [10.1109/JPHOT.2015.2489927](https://doi.org/10.1109/JPHOT.2015.2489927).
- [10] S. Rajagopal, R. D. Roberts, and S.-K. Lim, "IEEE 802.15.7 visible light communication: Modulation schemes and dimming support," *IEEE Commun. Mag.*, vol. 50, no. 3, pp. 72–82, Mar. 2012.
- [11] R. Singh, T. O'Farrell, and J. P. R. David, "An enhanced color shift keying modulation scheme for high-speed wireless visible light communications," *J. Lightw. Technol.*, vol. 32, no. 14, pp. 2582–2592, Jul. 2014.
- [12] A. E. Aziz, K. T. Wong, and J.-C. Chen, "Color-shift keying—How its largest obtainable "minimum distance" depends on its preset operating chromaticity and constellation size," *J. Lightw. Technol.*, vol. 35, no. 13, pp. 2724–2733, Jul. 2017.
- [13] R. X. G. Ferreira *et al.*, "High bandwidth GaN-based micro-LEDs for multi-Gb/s visible light communications," *IEEE Photon. Technol. Lett.*, vol. 28, no. 19, pp. 2023–2026, Oct. 2016.
- [14] S. Rajbhandari *et al.*, "A multigigabit per second integrated multiple-input multiple-output VLC demonstrator," *J. Lightw. Technol.*, vol. 35, no. 20, pp. 4358–4365, Oct. 2017.
- [15] 2017. [Online]. Available: <https://www.hhi.fraunhofer.de/en/departments/pn/technologies-and-solutions/hardware-products/vlc-system-1-gbits.html>
- [16] 2017. [Online]. Available: <http://purelifi.com/lifi-products/lifi-x/>
- [17] N. A. Riza, "Reconfigurable optical wireless," in *Proc. 12th Annual Meeting Lasers Electro-Opt. Soc.*, vol. 1, 1999, pp. 70–71, Paper no. MH4.
- [18] A. Gomez *et al.*, "Beyond 100-Gb/s indoor wide field-of-view optical wireless communications," *IEEE Photon. Technol. Lett.*, vol. 27, no. 4, pp. 367–370, Feb. 2015.
- [19] A. Gomez, C. Quintana, G. Faulkner, and D. C. O'Brien, "Point-to-multipoint holographic beamsteering techniques for indoor optical wireless communications," *Proc. SPIE*, vol. 9772, 2016, Paper no. 97720Q.
- [20] K. Wang, A. Nirmalathas, C. Lim, K. Alameh, and E. Skafidas, "Full-duplex gigabit indoor optical wireless communication system with CAP modulation," *IEEE Photon. Technol. Lett.*, vol. 28, no. 7, pp. 790–793, Apr. 2016.
- [21] A. M. J. Koonen, C. W. Oh, K. Mekonnen, Z. Cao, and E. Tangdionga, "Ultra-high capacity indoor optical wireless communication using 2D-steered pencil beams," *J. Lightw. Technol.*, vol. 34, no. 20, pp. 4802–4809, Oct. 2016.
- [22] M. Born and E. Wolf, *Principles of Optics: Electromagnetic Theory of Propagation, Interference and Diffraction of Light*, 7th ed. Cambridge, U.K.: Cambridge Univ. Press, 1999.
- [23] Z. Yaqoob, A. A. Rizvi, and N. A. Riza, "Free-space wavelength-multiplexed optical scanner," *Appl. Opt.*, vol. 40, no. 35, pp. 6425–6438, Dec. 2001.
- [24] C.W. Oh, E. Tangdionga, and A. M. J. Koonen, "Steerable pencil beams for multi-Gbps indoor optical wireless communication," *Opt. Lett.*, vol. 39, no. 18, pp. 5427–5430, Sep. 2014.
- [25] Z. Yaqoob, M. A. Arain, and N. A. Riza, "High-speed two-dimensional laser scanner based on Bragg gratings stored in photothermorefractive glass," *Appl. Opt.*, vol. 42, no. 26, pp. 5251–5262, Sep. 2003.
- [26] A. M. J. Koonen, C. W. Oh, and E. Tangdionga, "Reconfigurable free-space optical indoor network using multiple pencil beam steering," in *Proc. OptoElectron. Commun. Conf./Aust. Conf. Opt. Fibre Technol. 2014*, Melbourne, VIC, Australia, Paper no. Tu3F-1.
- [27] C. W. Oh, E. Tangdionga, and A. M. J. Koonen, "42.8 Gbit/s indoor optical wireless communication with 2-dimensional optical beamsteering," in *Proc. Opt. Fiber Commun. Conf. Exhib. 2015*, Los Angeles, CA, USA, Paper no. M2F.3.
- [28] T. Chan, E. Myslivets, and J. E. Ford, "2-Dimensional beamsteering using dispersive deflectors and wavelength tuning," *Opt. Express*, vol. 16, no. 19, pp. 14617–14628, Sep. 2008.
- [29] K. Van Acoleyen, W. Bogaerts, and R. Baets, "Two-dimensional dispersive off-chip beam scanner fabricated on silicon-on-insulator," *IEEE Photon. Technol. Lett.*, vol. 23, no. 17, pp. 1270–1272, Sep. 2011.
- [30] W. Guo, P. R. A. Binetti, C. Althouse, L. A. Johansson, and L. A. Coldren, "InP photonic integrated circuit with on-chip tunable laser source for 2D optical beam steering," in *Proc. Opt. Fiber Commun. Conf. Expo.*, Los Angeles, CA, USA, 2013, Paper no. OTh3I-7.
- [31] A. M. J. Koonen *et al.*, "2D beam-steered high-capacity optical wireless communication," in *Proc. IEEE Summer Top.*, Newport Beach, CA, USA, 2016, Paper no. TuC2.2.
- [32] A. M. Khalid, A. M. J. Koonen, C. W. Oh, Z. Cao, K. A. Mekonnen, and E. Tangdionga, "10 Gbps indoor optical wireless communication employing 2D passive beam steering based on arrayed waveguide gratings," in *Proc. IEEE Summer Top.*, Newport Beach, CA, USA, 2016, Paper no. TuC2.3.
- [33] A. M. J. Koonen, A. M. Khalid, C. W. Oh, F. Gomez-Agis, and E. Tangdionga, "High-capacity optical wireless communication using 2-dimensional IR beam steering," in *Proc. OptoElectron. Commun. Conf. 2017*, Singapore, Jul. 31–Aug. 4, 2017, Paper no. 1-4K-3.
- [34] 2017. [Online]. Available: <https://en.wikipedia.org/wiki/Etendue>
- [35] 2017. [Online]. Available: https://en.wikipedia.org/wiki/Nonimaging_optics
- [36] J. Zeng, V. Joyner, J. Liao, S. Deng, and Z. Huang, "A 5 Gb/s 7-channel current-mode imaging receiver front-end for free-space optical MIMO," in *Proc. 52nd IEEE Int. Midwest Symp. Circuits Syst. 2009*, Cancun, Mexico, pp. 148–151.
- [37] S. Collins, D. C. O'Brien, and A. Watt, "High gain, wide field of view concentrator for optical communications," *Opt. Lett.*, vol. 39, no. 7, pp. 1756–1759, Apr. 2014.
- [38] Z. Cao, L. Shen, Y. Jiao, X. Zhao, and A. M. J. Koonen, "200 Gbps OOK transmission over an indoor optical wireless link enabled by an integrated cascaded aperture optical receiver," in *Proc. Opt. Fiber Commun. Conf. 2017*, Los Angeles, CA, USA, Paper no. Th5A.6.
- [39] T.-H. Do and M. Yoo, "An in-depth survey of visible light communication based positioning systems," *Sensors*, vol. 16, no. 5, 2016, Paper no. 678. [Online]. Available: <http://www.mdpi.com/1424-8220/16/5/678>
- [40] N. Saha, M. S. Iftekhar, N. T. Le, and Y. M. Jang, "Survey on optical camera communications: Challenges and opportunities," *IET Optoelectron.*, vol. 9, no. 5, pp. 172–183, 2015.
- [41] N. T. Le, M. A. Hossain, and Y. M. Jang, "A survey of design and implementation for optical camera communication," *Signal Process. Image Commun.*, vol. 53, pp. 95–109, 2017.
- [42] J. Herrnsdorf, M. J. Strain, E. Gu, R. K. Henderson, and M. D. Dawson, "Positioning and space-division multiple access enabled by structured illumination with light-emitting diodes," *J. Lightw. Technol.*, vol. 35, no. 12, pp. 2339–2345, Jun. 2017.
- [43] A. M. Khalid *et al.*, "Bi-directional 35-Gbit/s 2D beam steered optical wireless downlink and 5-Gbit/s localized 60-GHz communication uplink for hybrid indoor wireless systems," in *Proc. Opt. Fiber Commun. Conf. Exhib. 2017*, Los Angeles, CA, USA, Mar. 2017, Paper no. Th1E.6.
- [44] K. A. Mekonnen, N. Calabretta, E. Tangdionga, and A. M. J. Koonen, "High-capacity dynamic indoor network utilizing optical wireless and 60-GHz radio techniques," in *Proc. Int. Top. Meeting Microw. Photon. 2017*, Beijing, China, Oct. 2017, Paper no. We.2.3.
- [45] A. Gomez, K. Shi, C. Quintana, G. Faulkner, B. C. Thomsen, and D. C. O'Brien, "A 50 Gb/s transparent indoor optical wireless communications link with an integrated localization and tracking system," *J. Lightw. Technol.*, vol. 34, no. 10, pp. 2510–2517, May 2016.
- [46] C.W. Oh, Z. Cao, E. Tangdionga, and A. M. J. Koonen, "10 Gbps all-optical full-duplex indoor optical wireless communication with wavelength reuse," in *Proc. Opt. Fiber Commun. Conf. Exhib. 2016*, Anaheim, CA, USA, Paper no. Th4A.6.
- [47] F. Gomez-Agis, S. van der Heiden, C. M. Okonkwo, E. Tangdionga, and A. M. J. Koonen, "112 Gbit/s transmission in a 2-D beam steering AWG-based optical wireless communication system," in *Proc. Eur. Conf. Opt. Commun. 2017*, Gothenburg, Sweden, Paper no. Th.2.B.1.

Ton Koonen (F'07) is a Full Professor with the Eindhoven University of Technology (TU/e) since 2001. Since 2004, he is the Chairman of the group Electro-Optical Communication Systems, and since 2012 the Vice-Dean of the Department of Electrical Engineering. Since 2016, he is also Scientific Director of the Institute for Photonic Integration at TU/e. Before 2001, he was involved in applied research in industry for more than 20 years, among others in Bell Labs - Lucent Technologies. His current research interests include optical fiber-supported in-building networks (including optical wireless communication techniques, radio-over-fiber techniques, and high-capacity plastic optical fiber techniques), optical access networks, and spatial division-multiplexed systems. Ton Koonen is a Bell Labs Fellow (1998), OSA Fellow (2013), and Distinguished Guest Professor of Hunan University, Changsha, China (2014). In 2011, he was recipient of an Advanced Investigator Grant of the European Research Council on optical wireless communication.